Nucleation and growth of Si/Si(111) observed by scanning tunneling microscopy during epitaxy

Bert Voigtländer and Thomas Weber
Institut für Grenzflächenforschung und Vakuumphysik, Forschungszentrum Jülich, 52425 Jülich, Germany
(Received 14 March 1996)

Si(111) homoepitaxy was studied with scanning tunneling microscopy (STM) during growth at high temperatures. The nucleation process on top of the epitaxially grown islands was directly observed with atomic resolution. The nucleation on the epitaxial layer occurs preferentially at domain boundaries of the 7×7 reconstruction. The high density of domain boundaries on the grown film and the low density of these surface defects on the original substrate lead to the observed multilayer growth for low coverages. At higher coverages, when the substrate is covered by the epitaxial layer, there is no longer a difference in the defect density in the different layers and the growth mode turns to layer growth. The layer distribution is directly measured with STM and can be described by simple rate equations. The high nucleation probability on top of the epitaxial layer results in an effective mass transport on top of the first-layer islands. [S0163-1829(96)04632-2]

The Si(111) homoepitaxy was studied by various methods in the recent years. Reflection high-energy electron diffraction[1,2] and high-resolution low-energy electron diffraction[3,4] experiments showed oscillations of the specular intensity that were attributed to a layer-by-layer growth mode. An initial transient in the observed intensity was attributed to a transition from initial double-layer growth mode to a layer-by-layer growth mode. Scanning tunneling microscopy (STM) experiments studied the details of the nucleation process occurring in the initial stages of growth and observed a multilayer growth mode for low coverages.[5] However, some issues could not be studied because no real-space method was available that could work during growth conditions (i.e., while evaporating and at high temperatures).

Recently, STM experiments during growth at high temperatures became feasible.[6–8] With such a method available, the nucleation process can be observed with atomic resolution during growth. On a larger scale, the ability to observe the same area during growth can be used to observe the transition from initial multilayer growth to layer-by-layer growth.

In this paper, we study the nucleation and growth processes during Si(111) homoepitaxy using the method of STM operation during growth at high temperatures, molecular-beam epitaxy scanning tunneling microscopy (MBESTM). The direct observation of the nucleation process showed that nucleation on epitaxially grown islands occurs preferentially at domain boundaries of the 7×7 structure. Also for larger coverages the growth process can be studied in detail because for any coverage the complete morphology of the growing film is measured during growth. From a statistical analysis of the data, the coverage in every layer is determined as a function of the total deposited amount and can be compared to predictions obtained from rate equations.

We used a beetle-type STM.[7,9] All piezos are surrounded by a shield for high-temperature operation and to prevent evaporation onto the piezos. The thermal drift is considerable when the sample temperature is raised. After 1 h at a fixed temperature (600–900 K) the thermal drift decreases to $\sim$10–20 Å/min. During scanning, we can correct for thermal drift. In successive images the same feature is marked and correction voltages are applied to the xy-scan signals to image the same surface area in successive images. The Si evaporator is located under an angle of 50° from the sample normal. Due to the open design of the scanning tunneling microscope, the molecular beam can be directed towards the sample, which is located in the scanning tunneling microscope position. Scanning is done continuously during growth. Part of the MBE beam impinging on the sample is shaded by the tip. With a typical tip radius of some hundred angstroms,[10] we use scan ranges of several thousand angstroms to minimize the fraction shaded by the tip. For recording images with atomic resolution, where the image size is only a few hundred angstroms, we use a slightly different technique. After completing a scan, we park the tip several hundred angstroms away from the scanned area for a while to allow the molecular beam to cover the total scanned area. Then the next image is scanned.

The MBESTM measurements were performed in an ultrahigh vacuum chamber (base pressure of 3×10^{-11} mbar). The Si(111) 7×7 substrates (1×10^{19} Sb atoms/cm^3 doping) were prepared by *in situ* thermal treatment. The STM images were taken in the constant current mode at sample bias voltages between 2.5 and -2.5 V and a tunneling current between 0.1 and 1 nA. Si was evaporated from a homemade electron-beam evaporator. Due to the crystallography of the Si(111) surface, the growth in the vertical direction occurs in units that are 3.1 Å high. We call this unit of 1.56×10^{15} atoms/cm^2 one monolayer, or 1 ML.

In Figs. 1(a)–1(h) sample images from a sequence of images of Si/Si(111) homoepitaxy are selected. The images were recorded at 700 K sample temperature in the presence of the Si beam with a rate of 0.07 ML/min at a frequency of $\sim$ 1 image/min. Si atoms from the vapor diffuse on the surface and nucleate in two-dimensional islands of triangular shape on the Si(111) substrate. A 7×7 domain boundary leads to preferred nucleation along a line [upper left to middle in the bottom of Fig. 1(a)]. At 0.8-ML coverage [Fig. 1(b), same area on the sample] the islands have grown and nucleation on top of the first-layer islands has occurred. In this stage, Si is clearly growing in a multilayer growth mode.

 © 1996 The American Physical Society

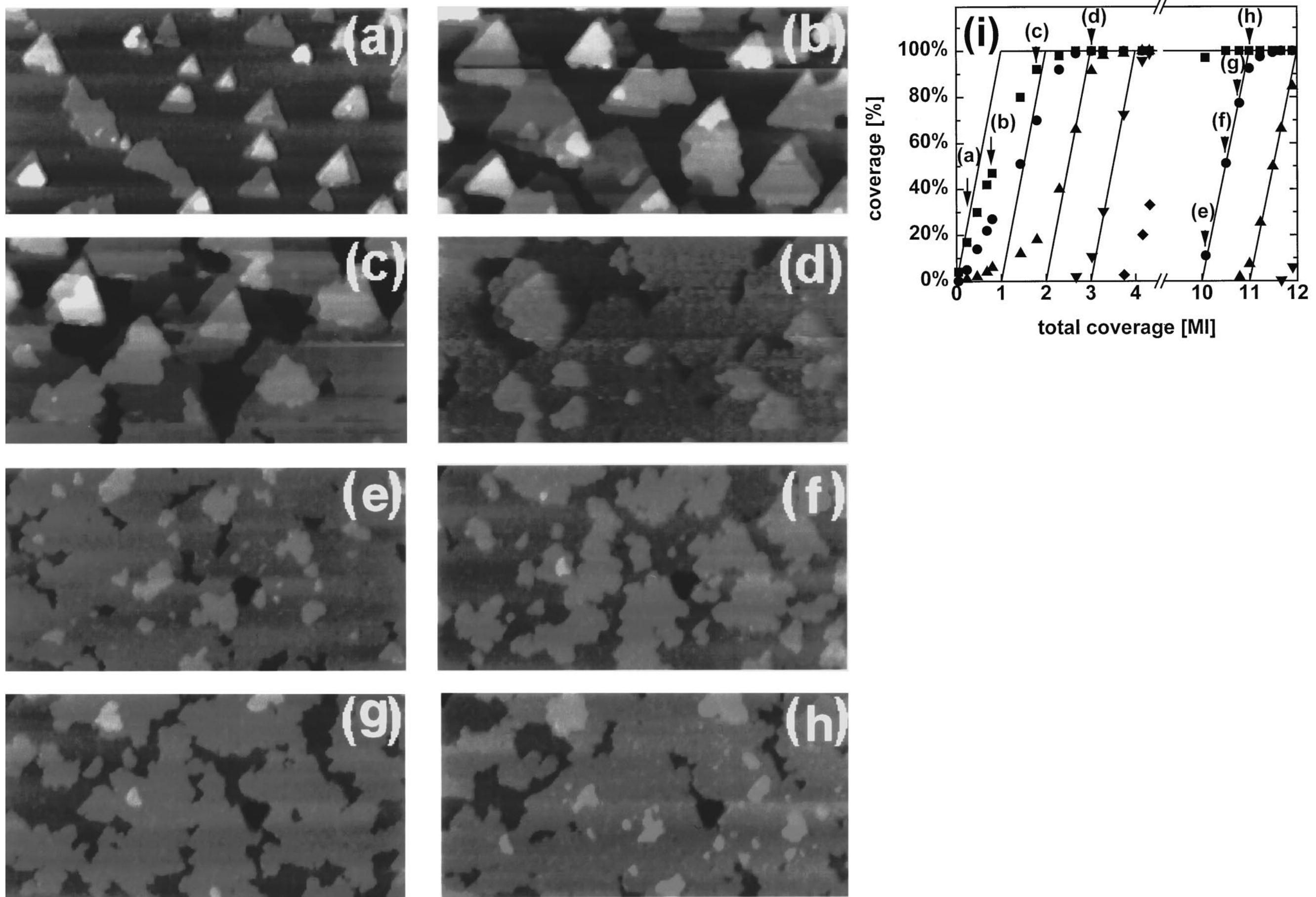

FIG. 1. Transition from initial multilayer growth to layer-by-layer growth in Si(111) homoepitaxy. STM images (2900 × 1400 Å^2) of the growth of Si on Si(111) at 700 K. Images (a)–(d) were recorded at 0.23-, 0.8-, 1.8-, and 3.0-layer Si coverage, respectively. One cycle of layer-by-layer growth is shown in (e)–(h). In (i) the coverage in each layer is plotted versus the total coverage. The data points corresponding to images (a)–(h) are indicated.

At 1.8-ML coverage [Fig. 1(c)] the islands coalesce and the substrate layer is nearly completely covered. At 3-ML coverage [Fig. 1(d)] a quite smooth film has formed. A transition from the initial multilayer growth to the layer-by-layer growth has occurred. For coverages higher than this, the growth mode stays close to the layer-by-layer growth mode. This can be seen in Figs. 1(e)–1(h), where sample images in a coverage regime from 10 to 11 ML are displayed. At 10-ML coverage [Fig. 1(e)] the ninth layer is almost closed and growth in the tenth layer has just nucleated. In Figs. 1(f)–1(g) the tenth layer closes and in Fig. 1(h) the surface morphology of the grown film looks quite similar to that in Fig. 1(e). (A triangular defect hole in the right part of the image can serve as a marker.)

In Fig. 1 a transition in the shape of the islands can be observed. Initially the form of the islands is triangular with the outward normal along the $[\bar{1}\,\bar{1}2]$ directions After coalescence and at higher coverages the form of the islands is more irregular [Figs. 1(d)–1(h)]. The facets of the initially triangular islands along the $[\bar{1}\,\bar{1}2]$ direction are known to be stable during growth[11,12] (we call the step edges of the two-dimensional islands facets). The growth of the $[11\bar{2}]$ facets that occur after coalescence of the triangular islands are known to be unstable and irregular steps occur.[11,12] This unstable growth along the $[11\bar{2}]$ facets is presumably the reason for the irregular shape of the islands during a later stage of growth.

One advantage of the MBESTM technique is that quantitative statistical analysis, such as, for instance, the amount of coverage in a certain layer as a function of the total deposited coverage, can be obtained in a single experiment. The conventional STM technique requires many separate snapshots at identical growth conditions to obtain such results as a function of coverage and additionally the influence of the quenching from growth temperature down to room temperature is unknown. In Fig. 1(i) the coverage in each layer is plotted versus the total coverage. Squares, circles, triangles, etc., indicate the coverage in the first, second, third, etc., layers, respectively. The solid lines indicate the expected behavior for ideal layer-by-layer growth, i.e., one layer is filled linearly up to 100% and only then the next layer starts to grow. For lower coverages the data show clear deviations from this ideal behavior. For instance, at 0.8-ML total coverage [Fig. 1(b)] the coverage in the first layer is 47%, the coverage in the second layer is 27%, and even some of the Si has nucleated in the third layer. Interestingly, this initial multilayer growth changes with further deposition to a mode very close to layer-by-layer growth. For coverages larger than 2.5 ML the measured coverages are very close to the solid lines indicating layer-by-layer growth. The rounded edges at the beginning and at the end of the completion of a monolayer arise due to nucleation in the next layer before the previous layer is completed. Apart from this detailed characterization of the growth on a nanometer length scale the ori-

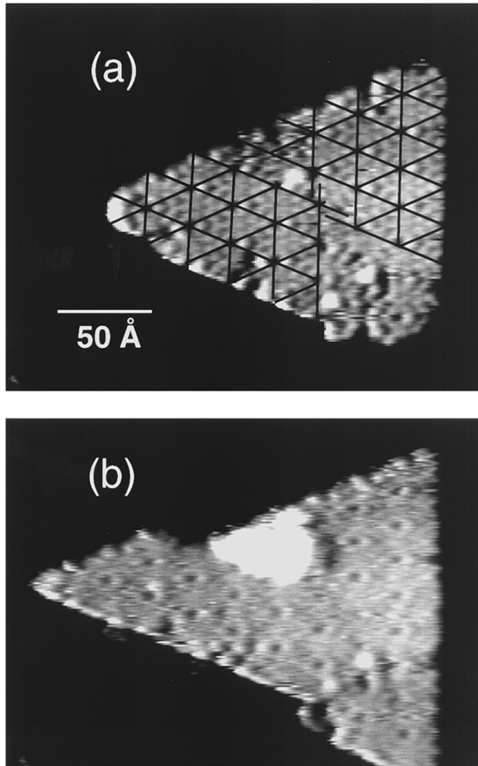

FIG. 2. STM image of a one-layer (3.1 Å) high island on Si(111) (the substrate is out of contrast and displayed in black) at a sample temperature of 670 K. Two domains of 7×7 (marked by grids) are visible and connected by a domain boundary. Upon Si evaporation nucleation of next layer growth occurs at this 7×7 domain boundary.

gin of this growth behavior on the atomic scale is an interesting topic.

Diffraction methods observed an anomaly in the diffracted intensity during the growth of the first two layers. STM experiments performed after growth showed preferred nucleation on top of monolayer high islands.[8] It was suggested that this preferred nucleation is caused by the higher surface defect density on the epitaxial layer. With the MBESTM technique it is possible to observe the nucleation process on top of the first-layer islands directly with atomic resolution during growth. Figure 2(a) shows an epitaxially grown Si island. The island has a height of 3.1 Å above the substrate (the substrate is out of contrast, shown in black in Fig. 2). On top of this island, we observe the characteristic dimer adatom stacking fault reconstruction. In the right and in the left part of the island, we observe two areas with 7×7 reconstruction indicated by grids. The two domains do not match (as indicated by the mutually shifted grids). They are connected by a domain boundary. In the lower right in Fig. 2(a) a more disordered region is observed. The observation of the domain boundary and the disordered region shows that a high density of surface defects is present on the epitaxial islands.[5] Figure 2(b) shows the same island as in Fig. 2(a) at a later stage during growth. We observe that just at the 7×7 domain boundary the growth of the next layer nucleates [white area in Fig. 2(b)]. This experiment proves directly that the domain boundaries on top of the epitaxial islands serve as preferred nucleation centers for second-layer growth. Such an experiment, i.e., to observe the growth history of an island as function of coverage, can be performed only by the MBESTM technique.

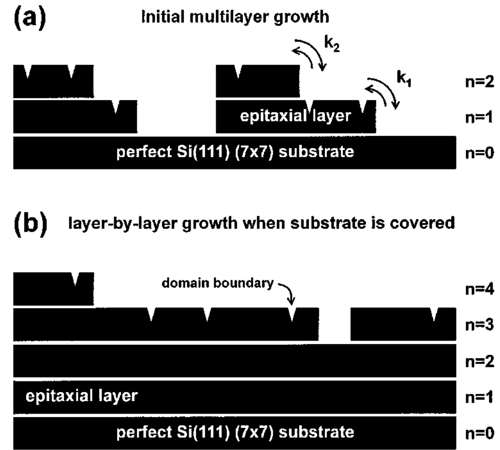

FIG. 3. Initial multilayer growth caused by the different defect density on the original substrate and on the epitaxial layer. The original substrate is almost free of surface defects. (a) Si nucleates at the domain boundaries, frequently occurring on top of the epitaxial layer, leading to multilayer growth. (b) Once the original substrate is covered by the epitaxial layer all layers have the same defect structure and the growth mode changes to layer-by-layer growth.

This preferential nucleation at the domain boundaries on the epitaxially grown layer is the reason for the initial multilayer growth. The observed transition from the initial multilayer growth to layer-by-layer growth is caused by the different structure of the original substrate and the epitaxial layer. The Si(111) substrate is a well-annealed surface with a very regular long-range 7×7 periodicity, only rarely disturbed by domain boundaries, whereas the epitaxial Si layer grown at relatively low temperature (670 K) has a high density of surface defects. When the substrate is only partly covered by the epitaxially grown layer, two different types of the Si terminated surfaces exist: the well-ordered substrate and the Si islands with a high density of domain boundaries [Fig. 3(a)]. These surface defects serve as nucleation centers on top of the epitaxial layer and lead to preferred nucleation of Si in the second layer. This nucleation on top of the epitaxial layer causes the multilayer growth in the beginning. However, when all of the substrate is completely covered with evaporated Si, the same defect density is found in all layers and no preferred nucleation in the upper layers occurs [Fig. 3(b)]. A transition to layer-by-layer growth is observed.

In the following, we compare the measured layer coverage [Fig. 1(i)] with the results of simple rate equations. A set of differential equations for the coverage in the nth layer θ_n can be written down:[13]

$$d\theta_n/dt=(1/\tau)(\theta_{n-1}-\theta_n)+(\text{net jumps from } n+1 \text{ to } n) -(\text{net jumps from } n \text{ to } n-1). \quad (1)$$

In equation (1) τ is the time to grow 1 ML and $n=0$ corresponds to the substrate. In a simple approach the jump rate for jumps from layer $n+1$ to layer n is proportional to the product of the available space on level n and the uncovered area on level $n+1$,[13] as indicated in Fig. 3(a). Equation (1) becomes

$$d\theta_n/dt = (1/\tau)(\theta_{n-1}-\theta_n)+k_n(\theta_{n+1}-\theta_{n+2})(\theta_{n-1}-\theta_n) - k_{n-1}(\theta_{n-1}-\theta_n)(\theta_{n-2}-\theta_{n-1}). \quad (2)$$

This set of differential equations is solved numerically and the rate constants k_n, which fit the experimental data best, can be determined. Large values of k_n give rise to an effective mass transport from higher layers to lower layers. The special cases are $k_n=\infty$ for layer-by-layer growth, $k_n=0$ (for all n) for growth without interlayer mass transport,[13] and $k_n<0$ for three-dimensional growth (i.e., mass transport from lower layers to higher layers). For total coverages greater than 3 ML the growth behavior becomes quite close to layer-by-layer growth and $k_n=30$ (for all n) fits the experimental data well in the coverage regime above 3 ML. During the growth of the first three layers the experimentally observed preferred nucleation on the epitaxial layer is expected to reduce the mass transport from the second to the first layer. Therefore a rate constant $k_1<30$ is expected. We found that a coverage-independent rate constant for the mass transfer between the second and the first layer (k_1) cannot explain the observed layer coverage. Physical arguments can be used to guess the coverage-dependence of this rate constant. Preferred nucleation on top in the first layer should be strongest for low coverages, where the most favorable binding sites at the domain boundaries are all available. For higher coverages, the energetically most favorable binding sites are already occupied and the jump rate down to the first layer should be higher. The simplest assumption is a linear increase of the rate constant k_1 as a function of θ_1. A quite good fit of the data points in the whole coverage regime can be obtained with $k_1=-5+9\theta_1$. This fit is shown as a solid line in Fig. 4 together with the data.

Values of $k_1<0$ occurring in the low-coverage regime indicate an effective upward mass transport from the first to the second layer due to the preferred nucleation in upper layers. This upward mass transport shows also that there is no significant Schwoebel barrier in the Si/Si(111) system. The tendency for an upward mass transport is also visible when we look at individual islands. For instance, in Fig. 1(b) there are several islands that are almost completely two monolayers high. This leads to the assumption that adatoms arriving from the vapor sample a quite large area (also jumping on top of islands) before they bond to the lowest-energy configuration. In this case the tendency towards multilayer growth can be predicted for different growth conditions. For near equilibrium growth conditions (i.e., high temperature or low deposition rate) the diffusing atoms sample the surface quite efficiently and bond to the lowest-energy sites (domain boundaries). This should give rise to an enhanced tendency towards multilayer growth. On the other hand, under kinetically limited growth conditions (i.e., at low temperature or high deposition rate) the tendency towards multilayer growth should be weaker. Experiments at different growth conditions show indeed that the tendency towards multilayer growth is weaker at higher deposition rates. Experiments performed at 675 K (0.2 ML of silicon deposited) showed that at a rate of 0.16 ML/min only 18% of the deposited material is in the second layer, while at the lower growth rate of 0.01 ML/min 27% of the material is in the second layer.

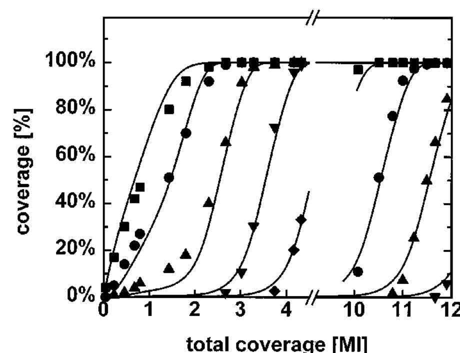

FIG. 4. Transition from initial multilayer growth to layer-by-layer growth described by simple rate equations (solid lines). The measured layer coverage is indicated by the data points. The fitted rate constants indicate an effective upward mass transport from the first to the second layer.

In conclusion, we have shown that the MBESTM technique makes it possible to study the nucleation at domain boundaries during Si(111) epitaxy with atomic resolution. This preferred nucleation on top of the epitaxial layer leads to initial multilayer growth. On a larger length scale the complete surface morphology is recorded during growth and can be analyzed in terms of layer coverage and other characteristics of interest. The measured layer coverage can be described by simple rate equations. The parameters entering in this rate equations show that the high nucleation probability on top of the islands leads to an effective upward mass transport in the submonolayer coverage regime.

T. Sakamoto, N.J. Kawai, T. Nakagawa, K. Ohta, and T. Kojima, Appl. Phys. Lett. **47**, 617 (1985).

[1] M. Ichikawa and T. Doi, Appl. Phys. Lett. **50**, 1141 (1987).

[2] R. Altsinger, H. Busch, M. Horn, and M. Henzler, Surf. Sci. **200**, 235 (1988).

[3] M. Horn-von Hoegen and H. Pietsch, Surf. Sci. **321**, L129 (1994).

[4] U. Köhler, J.E. Demuth, and R.J. Hamers, J. Vac. Sci. Technol. A **7**, 2860 (1989).

[5] T. Hasegawa, M. Kohno, S. Hosaka, and S. Hosoki, Phys Rev. B **48**, 1943 (1993).

[6] B. Voigtländer and A. Zinner, Appl. Phys. Lett. **63**, 3055 (1993).

[7] U. Köhler, L. Andersohn, and B. Dahlheimer, Appl. Phys. A **57**, 491 (1993).

[8] J. Frohn, J.F. Wolf, K. Besocke, and M. Teske, Rev. Sci. Instrum. **60**, 1200 (1989).

[9] J.P. Ibe *et al.*, J. Vac. Sci. Technol. A **8**, 3570 (1990).

[10] R.T. Tung and F. Schrey, Phys. Rev. Lett. **63**, 1277 (1989).

[11] W. Shimada and H. Tochihara, Surf. Sci. **311**, 107 (1994).

[12] P.I. Cohen, G.S. Petrich, P.R. Pukite, G.J. Whaley, and A.S. Arrott, Surf. Sci. **216**, 222 (1989).